Section A-Research paper

Isolation of undescribed flavonoid glycoside from *Hibiscus calyphyllus* flowers and their antitubercular activity

Manju Thalaimalai [1,2], Jeyachandran Malaichamy [2*], Dharmarajan Sriram[3]

[1] Research Scholar (Reg. No.19211232032003), Department of Chemistry & Research Centre, Sri Paramakalyani College, (Aff. To Manonmaniam Sundaranar University, Tirunelveli), Alwarkurichi – 627412, Tamil Nadu, India.

[2*] Department of Chemistry & Research Centre, Sri Paramakalyani College, Alwarkurichi – 627412, Tenkasi, Tamil Nadu, India, E. mail: jeyachandranm@gmail.com.

[3] Birla Institute of Technology & Science-Pilani, Hyderabad Campus, Jawahar Nagar, Hyderabad- 500 078, India.

ABSTRACT

Isolation of an undescribed flavonoid glycoside from the flowers of *H. calyphyllus* characterised as 2-(3,4-dihydroxyphenyl)-3,5,7-trihydroxy-8-{(3,4,5-trihydroxy-6-(hydroxymethyl)tetrahydro-2*H*-2-pyranyl)oxy}-4*H*-4-chromenone, **I**. The structure was clearly assigned through UV, IR, 1D, 2D-NMR and MS studies. Compound **I** showed influential antitubercular activity (MIC = 0.05 µg/mL) against MTB H37Rv. Distinctively, compound **I** showed fifteen times more active than Ethambutol (MIC = 1.56 µg/mL); four times more active than Rifampicin (MIC = 0.2 µg/mL) and two-times more active than the standard drug Isoniazid (MIC = 0.1 µg/mL).

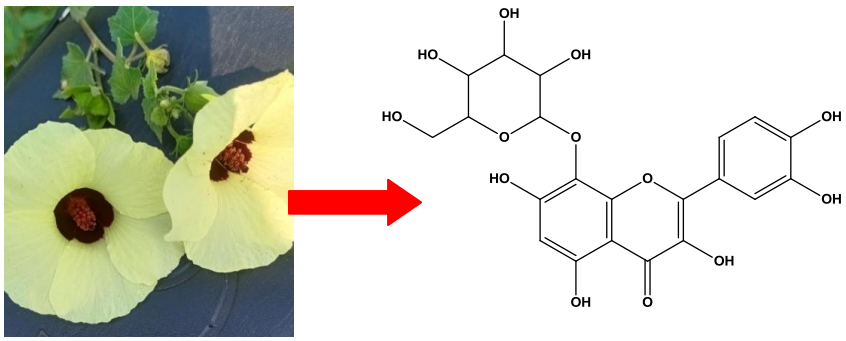

Key words: *Hibiscus calyphyllus*, Flavonoid glucoside, Spectroscopic studies, Antitubercular activity.

1. Introduction

Hibiscus calyphyllus (Malvaceae) is a ubiquitous perennial plant and is commonly recognized as lemon-yellow rosemallow. The leaves of the plant are used as a food and also used as medicine for sores. Roots can be used as a remedy for pneumonia.[1] People of Uganda poles used the stems for building, Tanzanians made bast fibre and Kenyan used the leaves for dressing the wounds.[2] Moreover, *H. calyphyllus* is cultivated throughout the tropics and subtropics as an ornamental. The plant parts are also used to produce oils.[3] The fractions of *H. calyphyllus* possess antioxidant, cytotoxic, antidiabetic, and antiobesity properties.[4,5] However, there is no report on the phytochemical evaluation on *H. calyphyllus* leads us to evaluate the phytochemical constituents present in this plant. And the objectives of the present study were intend to explore the secondary metabolites from the flowers of *H. calyphyllus,* and to elucidate the structure through UV, IR, 1D NMR, 2D NMR and LC-ESIMS studies. In our ongoing conquest of discovery newer drugs for limiting the TB,[6-8] the present study was planned to analyze antitubercular activity of isolated compound from *H. calyphyllus* flowers.

2. Materials and Methods

The melting point was determined in open capillary tubes and is uncorrected. UV spectra were recorded on HITACHI UH5300 UV-Vis spectrophotometer. The IR spectrum was recorded on Thermofisher Nicolet IS5R FT-IR KBr windows with a diamond crystal plate spectrometer. NMR spectra were recorded on a Bruker Avance 400 MHz FT-NMR spectrometer. The chemical shifts are reported in ppm downfield from tetramethylsilane. LC-ESIMS was analysed on Agilent 6530 LC/Q–TOF LC–MS spectrometer. The homogeneity of the compound was checked by TLC. For preparative TLC, Silica gel G Loba Chemie Pvt. Ltd. were coated on glass substrates (20 cm x 20 cm) using DD water and the solvent was removed in hot air oven.

3. Experimental

3.1. Plant Material

H. calyphyllus flowers were collected from Pottal Pudur (8°47'29.4"N 77°23'40.3"E), Tenkasi district of Tamil Nadu, India in month of January 2021 and were authenticated by Dr. K. Petchimuthu, Taxonomist, Sri KGS Arts College, Srivaikundam.

3.2. Extraction and isolation

About 500 g of the flowers of *H. calyphyllus* were collected and were immersed with 1 L ethanol for one week. The extract was filtered and the solvent was removed *in vacuo* afforded the 32 g brown pasty mass of the crude extract. It was stored in refrigerator for further analysis.

3.3. Fractionation

The extract (25 g) was mixed with 20 mL of hot ethanol and 50 g of silica gel for column chromatography 60-120 mesh to get slurry. The slurry was dried and packed in soxhlet extractor and were consecutively re-extracted with different solvents namely hexane, chloroform, ethyl acetate, dichloromethane and ethanol. Each of the re-extracts obtained from the different solvents were concentrated in rotary evaporator and then stored in refrigerator for further analysis. The chloroform re-extract (4.2 g) answered positive Shinoda test for flavonoids and it is found to be a mixture in TLC. The examination of TLC using neutral ferric chloride spraying agent also give the positive test for the presence of polyphenolic compounds.. Then the extract was dissolved in chloroform and applied on preparative TLC plates (34 numbers) and which was developed in chloroform and ethyl acetate mixture in the ratio of 8 : 2. After the development of the plates, which were allowed to dry and viewed with a naked eye shows five different bands. Among these, 27 plates showed the yellow colour bands (Rf value 0.43) and were scraped out with a razor blade. The yellow mass (3.1 g) obtained from the above was extracted into soxhlet apparatus using methanol (100 mL) and the solvent was removed *in vacuo* afforded 25 mg of compound **1** (Fig. **1**) as yellow powder.

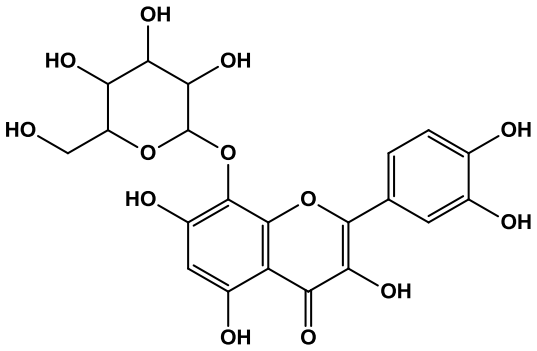

Fig. 1. Compound **1**.

3.4. Antituberculosis activity using MABA assay

The Microplate Alamar Blue Assay (MABA) to determine the MIC (minimum inhibitory concentration) of compounds against *Mycobacterium tuberculosis* H37Rv was tested. Serial two-fold dilutions of each drug were prepared directly in a sterile 96-well microliter plate using 100 µL 7H9-S. A growth control containing no antibiotic and a sterile control were also prepared on each plate. Sterile water was added to all perimeter wells to avoid evaporation during the incubation. The plate was covered, sealed in plastic bags and incubated at 37 ^{o}C in normal atmosphere. After 7 days incubation, 30 µL of alamar blue solution was added to each well, and the plate was re-incubated overnight. A change in colour from blue (oxidised state) to pink (reduced) indicated the growth of bacteria, and the MIC was defined as the lowest concentration of drug that prevented this change in colour.[9-10]

4. Results and Discussion

Characterization of Compound 1

Amorphous yellowish powder, m.p., 228 ^{o}C.

4.1. UV – Vis Spectra and shift reagents

The use of UV-Vis shift reagents has proven to be very useful in determining the substitution patterns.[11,12] Methanolic solution of compound **1** produces band I maxima at 382 nm. The use of sodium acetate, a weaker base ionizes the most acidic C-7 hydroxyl group and the absorption shifts to 5 nm (387 nm). Aluminium chloride forms complex between the C-4 carbonyl group and either 3-OH or 5-OH group and produces hypsochromic shift to 5 nm (377 nm). Upon

addition of HCl into the $AlCl_3$ complex the absorption shifts 4 nm (381 nm) that suggests that the above formed complex is unstable in acid and the shift may be due the *othro*-system of hydroxyl-groups in ring B is not stable after addition of HCl. Sodium hydroxide solution also produces hypsochromic shift to 42 nm (340) due the ionization of all phenolic hydroxyl groups. Additionally shift reagents of sodium methoxide shifts on absorption band at 52 nm, water and acetic acid observes the hypsochromic shift at 10 nm and 7 nm respectively. The versatile shift reagents used and their absorption are represented in **Table 1.**

Table 1: UV-Vis spectral characteristics of Compound 1 with versatile shift reagents

Solvent	**λ_{max} (nm)**
MeOH	382
MeOH + NaOAc	325, 387
MeOH + $AlCl_3$	377
MeOH + $AlCl_3$+ HCl	381, 787
MeOH + NaOH	340
MeOH + NaOMe	330
Water	372
Acetic acid	375, 787

4.2. IR Spectra

IR υ_{max}*:* 3494 (OH str.), 3170, 1648 (C=O str.), 1565, 1438, 1272, 1044, 991, 850, 708, 575 cm^{-1}. The absorption bands at 3494 cm^{-1} is due to OH str. and at 1648 $cm^{-1}$is owing to C=O str.

4.3. 1D and 2D NMR Spectra

^{1}H NMR (400 MHz, DMSO-d_6) δ ppm: 3.23-3.40 (m, 2H, glucosyl protons), 3.42 (t, 1H, J = 8.4 Hz, 8.4 Hz, 4”-H), 3.60 -3.70 (m, 2H, 6”-C$\underline{H_2}$), 4.66 (d, J = 8 Hz, 1H, 2”-H), 4.76 (t, J = 10.4 Hz

, 2.8 Hz, 1H, 3”-H), 5.02 (d, J = 5.2 Hz, 1H, 5”-H), 5.27 (d, J = 4.8 Hz, 1H, 6”-H), 6.27 (s, 1H, 6-H), 6.91 (d, 1H, J = 8.4 Hz, 5’-H), 7.82 (dd,1H, J = 8.4 Hz, 2.0 Hz, 6’-H), 7.90 (d, J = 2.0, 1H, 2’-H), 9.28 (bs, 1H, 3-OH), 9.43 (bs, 1H, 7-OH), 9.55 (bs, 1H, 3’-OH), 12.36 (s, 1H, 5-OH); *^{13}C NMR (100 MHz, DMSO-d_6) δ ppm:* 60.86 (C$\underline{H}_2$ -6”), 69.54 (C-5”), 74.53 (C-3”), 76.36 (C-4”), 77.56 (C-6”), 98.72 (C-6), 103.38 (C-10), 106.88 (C-2”), 115.95 (C-2’), 116.08 (C-5’), 121.41 (C-6’), 122.51 (C-1’), 125.58 (C-8), 136.17 (C-3), 145.24 (C-4’), 147.66 (C-3’), 148.24 (C-2), 148.74 (C-5), 156.75 (C-9), 156.85 (C-7), 176.33 (C-4, -C=O); *DEPT 135 (DMSO-d_6) δ ppm:* 60.87 (C$\underline{H}_2$-6”), 69.55 (C-5”), 74.54 (C-3”), 76.37 (C-4”), 77.56 (C-6”), 98.72 (C-6), 106.88 (C-2”), 115.95 (C-2’), 116.08 (C-5’), 121.41 (C-6’). HMBC correlation of compound I is represented in Fig.**2**.

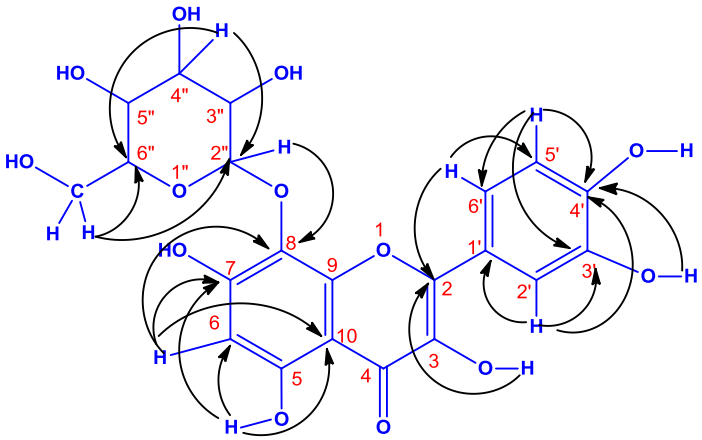

Fig. 2. HMBC Correlation of Compound **1**.

In the ^{1}H NMR spectra of compound **1**, a multiplet at δ 3.23 - 3.40 ppm is due to the glycosyl protons, and the 4”-H appears as a triplet at δ 3.42 ppm. A multiplet at δ 3.60 – 3.70 ppm is ascribed to 6” methylene group. The doublets at δ 4.66, 5.02, 5.27, 6.91 and 7.90 ppm are due to 2”, 5”, 6”, 5’ and 2’ methine protons respectively. The 3” proton appears as a triplet at δ 4.76 ppm. The singlets at δ 6.27 and 12.36 ppm is due to 6-C$\underline{H}$ and 5-O$\underline{H}$ respectively. The 3, 7 and 3’ hydroxyl protons of appears as a broad singlets at δ 9.28, 9.43 and 9.55 ppm respectively. A doublet of doublet at δ 7.82 is due to 6’ proton.

Carbons are assigned on the basis of C-H COSY, DEPT-135 and HMBC spectral data. The C-4 carbonyl carbon appears at δ 176.33 ppm. The negative peak in DEPT-135 at δ 60.87 ppm is attributed to C-6” methylene carbon; the nine positive peaks are due to methine carbons of C-6,

C-2' , C-5', C-6', C-2", C-3", C-4", C-5" and C-6". In 2D NMR, the C-3 hydroxyl proton is coupled with C-2, while C-5 hydroxyl proton is coupled with C-6, C-10 and C-7 carbon atoms. Similarly, C-6 hydrogen is coupled with C-10, C-8 and C-7 carbons; the proton of C-2' is coupled with C-1', C-4' and C-3' carbons. Moreover, the hydroxyl proton of C-3' is coupled with C-4' carbon; the proton of C-5' is coupled with C-6', C-4' and C-3' carbons; the proton of C-2" is coupled with C-8 carbon. The proton of C-6' is coupled with C-5' and C-2 carbons. Further, the proton of C-4" is coupled with C-6" and C-2" carbons; the protons of 6" methylene hydrogens are coupled with C-2" and C-6" carbons. From the above data we concluded that the obtained product is 2-(3,4-dihydroxyphenyl)-3,5,7-trihydroxy-8-{(3,4,5-trihydroxy-6-(hydroxymethyl)tetrahydro-2*H*-2-pyranyl)oxy}-4*H*-4-chromenone (**Fig. 1**). Characterization of 1D and 2D NMR spectra of Compound **1** is represented in **Table 2.**

Table 2: 1D and 2D NMR spectra of Compound 1

	C-H COSY & HMBC data	
Position	**^{13}C**	**HMBC**
3-O<u>H</u> (9.28)	136.17 (C-3)	148.24 (C-2)
5-O<u>H</u> (12.36)	148.74 (C-5)	98.72 (C-6), 103.38 (C-10), 156.85 (C-7)
6-H (6.27)	98.72 (C-6)	103.38 (C-10), 125.58 (C-8), 156.85 (C-7)
2'-H (7.90)	115.95 (C-2')	122.51 (C-1'), 145.24 (C-4'), 147.66 (C-3')
3'-O<u>H</u> (9.43)	147.66 (C-3')	145.24 (C-4')
5'-H (6.91)	116.08 (C-5')	121.41 (C-6'), 145.24 (C-4'), 147.66 (C-3')
6'-H (7.82)	121.41 (C-6')	116.08 (C-5'), 148.24 (C-2)
2"-H (4.66)	106.88 (C-1")	125.58 (C-8)
4"-H (3.42)	76.36 (C-3")	77.56 (6"-C), 106.88 (2"-C)
6"-C<u>H$_2$</u> (3.60)	60.86 (C-6")	106.88 (C-2"), 77.56 (C-6")

4.4. Mass spectra

LCESIMS [M-H]- m/z 480.0845 (calcd. for 480.09).

From the above spectral data, the structure of the compound **1** is assigned as 2-(3,4-dihydroxyphenyl)-3,5,7-trihydroxy-8-{(3,4,5-trihydroxy-6-(hydroxymethyl)tetrahydro-2*H*-2-pyranyl)oxy}-4*H*-4-chromenone.

4.5. Antitubercular activity

Compound **I** showed influential antitubercular activity (MIC = 0.05 μg/mL) against MTB H37Rv in comparison with Isoniazid, Rifampicin and Ethambutol. Specifically, compound **I** showed fifteen times more active than Ethambutol (MIC = 1.56 μg/mL); four times more active than Rifampicin (MIC = 0.2 μg/mL) and two-times more active than the standard drug Isoniazid (MIC = 0.1 μg/mL).

5. Conclusion

In conclusion, we have isolated an undescribed flavonoid glycoside from the flowers of *H. calyphyllus* characterised as 2-(3,4-dihydroxyphenyl)-3,5,7-trihydroxy-8-{(3,4,5-trihydroxy-6-(hydroxymethyl)tetrahydro-2*H*-2-pyranyl)oxy}-4*H*-4-chromenone. And this is the first report on the isolation of compound **1** from *H. calyphyllus.* The structure was clearly assigned through UV, IR, 1D, 2D-NMR and MS studies. Compound **I** showed promised antitubercular activity compared to the standard drugs i.e., fifteen times more active than Ethambutol; four times more active than Rifampicin and two-times more active than the standard drug Isoniazid.

Acknowledgement

The authors are thankful to Dr D. Shriram, BITS-Pilani, Hyderabad Campus for the antitubercular studies and DST FIST instrumentation facility for Sri Paramakalyani College.

Conflicts of Interest

The authors declare no conflict of interest.

References

1. Ruffo, C. K., Birnie, A., Tengnas, B., 2002.Technical Handbook No. 27, Edible Wild Plants of Tanzania by RELMA Technical Handbook series, Regional Land Management Unit, Sida, ICRAF House, Gigiri, Kenya, ISBN 9966-896-62-7, pp-362-363.
2. Bosch, C.H. 2004. Hibiscus calyphyllus Cav. PROTA (Plant Resources of Tropical Africa), Wageningen, Netherland, http://www.prota4u.org/search.asp (accessed 19 March 2023).
3. Alnadif, A. M., Mirghani, M. S., Hussein, I. 2017. Unconventional Oilseeds and Oil Sources, first ed., Academic Press, London.
4. Siddiqui, N. A., AI Yousef, H. M., Alhowiriny, T. A., Alam, P., Hassan, W. H. B., Amina, M., Hussain, A., Abdelaziz, S., Abdallah, R, H., 2018. Anticancer activity and concurrent analysis of ursolic acid, β-sitosterol and lupeol in three different Hibiscus species (aerial parts) by validated HPTLC method. Saudi Pharm J. 26 (2), 266–273. https://doi.org/10.1016/j.jsps.2018.05.015
5. Al-Yousef, H. M., Hassan, W. H. B., Abdelaziz, S., Amina, M., Adel, R., El-Sayed, M., A., 2020. UPLC-ESI-MS/MS Profile and Antioxidant, Cytotoxic, Antidiabetic, and Antiobesity Activities of the Aqueous Extracts of Three Different Hibiscus Species. Journal of Chemistry, 2020, Article ID 6749176, 17 pages, https://doi.org/10.1155/2020/6749176
6. Jeyachandran, M., Ramesh, P., Sriram, D., Senthilkumar, P., Yogeeswari, P. , 2012. Synthesis and in vitro antitubercular activity of 4-aryl/alkylsulfonylmethylcoumarins as inhibitors of *Mycobacterium tuberculosis*. Bioorg. Med. Chem. Letters. 22, 4807-4809. https://doi.org/10.1016/j.bmcl.2012.05.054
7. Sarojini, P., Shriram, K., Jeyachandran, M., Krishna, V. S., Sriram, D., 2018. Identification of Novel Metabolites and Screening of Antimicrobial and Anti-mycobacterium tuberculosis Activity of Bauhinia Purpurea Flowers International Journal of Green and Herbal Chemistry. 7 (3), 328-335. DOI: 10.24214/IJGHC/HC/7/3/32835
8. Sarojini P., Ranganathan, P., Jeyachandran, M., Sriram, D., Gandhimathi, S, 2021. Facile microwave-assisted synthesis and antitubercular evaluation of novel aziridine derivatives. Journal of Molecular Structure, 1233 (5), 130038. https://doi.org/10.1016/j.molstruc.2021.130038

9. Collins L. A., Franzblau S. G., 1997. Microplate alamar blue assay versus BACTEC 460 system for high-throughput screening of compounds against *Mycobacterium tuberculosis* and *Mycobacterium avium*. Antimicrob. Agents Chemother. 41 (5), 1004-1009. https://doi.org/10.1128%2Faac.41.5.1004
10. Krishna, V.S., Zheng, S., Rekha, E.M., Guddat, L.W. and Sriram, D., 2019. Discovery and evaluation of novel *Mycobacterium tuberculosis* ketol-acid reductoisomerase inhibitors as therapeutic drug leads. Journal of computer-aided molecular design. 33 (3), 357-366. https://doi.org/10.1007/s10822-019-00184-1
11. Bajracharya, G. B., Paudel, M., Rajendran, K. C, 2017. Insight into the structure elucidation of flavonoids throughuv-visible spectral analysis of quercetin derivatives using shift reagents. J. Nepal Chem. Soc. 37, 55-64. https://doi.org/10.3126/jncs.v37i0.32147
12. Mabry, T. J., Markham, K. R., Thomas, M. B. 1970. The Ultraviolet Spectra of Flavones and Flavonols. In: The Systematic Identification of Flavonoids. Springer, Berlin, Heidelberg. https://doi.org/10.1007/978-3-642-88458-0_5.